

Field-dependent specific heat of polycrystalline $\text{YBa}_2\text{Cu}_3\text{O}_{7-x}$

M. E. Reeves, S. E. Stupp, T. A. Friedmann, F. Slakey, D. M. Ginsberg, and M. V. Klein
*Department of Physics and Materials Research Laboratory, University of Illinois at Urbana-Champaign,
 1110 West Green Street, Urbana, Illinois 61801*

(Received 21 February 1989)

We have measured the specific heat of high-purity, sintered $\text{YBa}_2\text{Cu}_3\text{O}_{7-x}$ powder. The sample was characterized by x-ray diffraction and Raman scattering. We measured its dc magnetic susceptibility as a function of magnetic field and temperature to verify its superconducting properties and found the transition temperature T_c to be 90 K. The heat capacity was determined between 2 and 10 K in magnetic fields up to 3 T. The low-temperature specific heat exhibited a linear term (with a zero-field coefficient of 4.37 mJ/mol K^2) and a cubic term (corresponding to a Debye temperature of 375 K) that varied with field. Raman-effect data obtained on our sample showed that less than one-third of the linear term could arise from the presence of BaCuO_2 . Using Ginzburg-Landau theory in the London limit, we calculated the field dependence of the specific heat of a uniaxially symmetric superconductor. We were unable to account for the reduction of the cubic term, and we were able to account for only part of the enhancement of the linear term with increasing field in terms of the kinetic energy of the electrons circulating around the magnetic vortices (fluxoids). Perhaps the reason that Ginzburg-Landau theory fails to account for our data is that the superconducting order parameter does not change slowly over a length characteristic of the atomic structure of this material.

I. INTRODUCTION

$\text{YBa}_2\text{Cu}_3\text{O}_{7-x}$ was the first compound to exhibit superconductivity above 77 K.¹ Besides having a high transition temperature, this material and the other rare-earth superconducting oxides in the same family, $\text{RBa}_2\text{Cu}_3\text{O}_{7-x}$, have anisotropic normal-state parameters and extremely high upper critical fields. While the high- T_c superconductors share many features of the lower- T_c ones, they differ from conventional superconductors in several striking ways.²

According to BCS theory, the low-temperature specific heat of the superconducting electrons should be proportional to $\exp(-\Delta/kT)$, where Δ is the superconducting energy gap. Thus, as the temperature approaches absolute zero, the electronic specific heat should quickly vanish. Defying this conventional behavior, samples of various high-temperature superconductors,³ including $\text{YBa}_2\text{Cu}_3\text{O}_{7-x}$, exhibit a linear term in the low-temperature heat capacity. These results have been summarized in a review article by Fisher, Gordon, and Phillips.⁴ Our heat capacity measurements, correlated with Raman effect and dc magnetic susceptibility measurements, all made on the same sample, support the classification of the linear term as an intrinsic property of $\text{YBa}_2\text{Cu}_3\text{O}_{7-x}$.

We have measured the heat capacity of a carefully made and well-characterized sample of $\text{YBa}_2\text{Cu}_3\text{O}_{7-x}$ at low temperatures and in magnetic fields up to 3 T. We see a linear term at low temperatures that is enhanced as we increase the field. This enhancement has already been predicted by the work of Maki⁵ and of Fetter and Hohenberg,⁶ we compare the increase in the linear term that we

see to their predictions. Using Ginzburg-Landau theory in the limit $H_{c1} \ll B \ll H_{c2}$ and for $T \ll T_c$, and taking the anisotropic nature of these materials into account, we have recalculated the expected enhancement of the specific heat in a magnetic field. The results for the linear term are still inconsistent with published values of the anisotropy and of the London penetration depth.

II. EXPERIMENTAL METHOD

A. Sample preparation

The interpretation of the specific heat data requires a detailed study of the impurities in the sample. Even small amounts of BaCuO_2 have been shown to contribute greatly to the linear term in the specific heat at low temperatures.⁷⁻⁹ We have made our samples carefully, and using x-ray diffraction and Raman-effect spectroscopy, we have measured the amounts and types of impurities present in them.

In a glove bag filled with nitrogen, powders of BaCO_3 , Y_2O_3 , and CuO (all 99.999% pure) were weighed, thoroughly mixed, and ground with an agate mortar and pestle. The mixture was heated in a platinum crucible in air at 950°C for 24 h, with two intermediate grindings. The reacted material was ground and pressed into 0.5-g pellets under a pressure of 500 MPa applied for 5 min, producing a sample with about 75% of the ideal density. After removal from the press, the pellets were placed on $\text{YBa}_2\text{Cu}_3\text{O}_{7-x}$ powder, which in turn rested on a platinum sheet. This arrangement of pellets, powder, and platinum was placed in a tube furnace and heated in a stream of pure oxygen at 1 atm. pressure. The heat treat-

ment lasted for 24 h at 900 °C, followed by a slow cool (12 °C/h) to room temperature.

We verified that the pellets were nearly single phase, using x-ray diffraction. We saw evidence of small amounts of Y_2BaCuO_5 (approximately 2 wt. %) and CuO (approximately 1 wt. %) but did not detect the presence of BaCuO_2 (to a sensitivity of roughly 1 wt. %). Because very small amounts of BaCuO_2 could account for the linear term we see in the heat capacity at low temperatures,^{7,8} we needed to check for the presence of this impurity more sensitively. The work of Rosen and Macfarlane¹⁰ shows that trace amounts of this impurity contribute greatly to the Raman spectra of $\text{YBa}_2\text{Cu}_3\text{O}_{7-x}$. Following the method described in their paper, we measured the Raman spectra of oxygen-enriched and oxygen-depleted samples.

We cut one of the $\text{YBa}_2\text{Cu}_3\text{O}_{7-x}$ pellets in half and heat treated each half in flowing gas at 800 °C for 24 h. One piece was placed in flowing O_2 , while the other was placed in flowing He. If the sample were contaminated with BaCuO_2 , the Raman spectra of the oxygen annealed sample would show a peak at 640 cm^{-1} . This peak would then disappear after annealing in helium.¹⁰

The Raman scattering was performed using the polarized 5145 and 4880 Å lines of an argon ion laser. The scattered light was dispersed by a triple-stage monochromator and detected by a nitrogen-cooled photomultiplier tube. Together these instruments provided a resolution of 3 cm^{-1} and a dark count of approximately 1 count/s. To ensure the homogeneity of the examined samples, the laser spot was focused to roughly 0.5 mm^2 and moved to different regions of the surface. The sample's homogeneity in depth was verified by scraping it and remeasuring the Raman spectrum.

The pellets annealed in oxygen and helium exhibited the Raman-active modes expected of an $\text{YBa}_2\text{Cu}_3\text{O}_{7-x}$ superconductor¹¹ as well as modes attributed to the Y_2BaCuO_5 "green" phase.¹⁰ However, the 640-cm^{-1} mode associated with impurities of BaCuO_2 (Ref. 10) could not be detected to within the sensitivity of the apparatus. Assuming a linear dependence of the intensity of the mode on the presence of the impurity, we compare our data to those of Rosen *et al.*¹⁰ and calculate that the maximum BaCuO_2 concentration possible in the sample is 0.3%.

B. Magnetic susceptibility

Once the purity of the sample had been checked, we investigated the sharpness of the superconducting transition by measuring its magnetic susceptibility with an SHE VTS150 susceptometer. The sample was placed in a no. 5 gelatin capsule and cooled to 5 K with the magnetic field set to zero. A field of 13.7 Oe was applied, and the magnetic moment of the sample was measured while warming the sample from 5 to 100 K. The data are shown in Fig. 1. The zero-field data have an accuracy of $\pm 10\%$ because the zero-field condition is measurable by our apparatus only to within an accuracy of 1 Oe. The superconducting transition looks sharp except for a knee near 60 K.

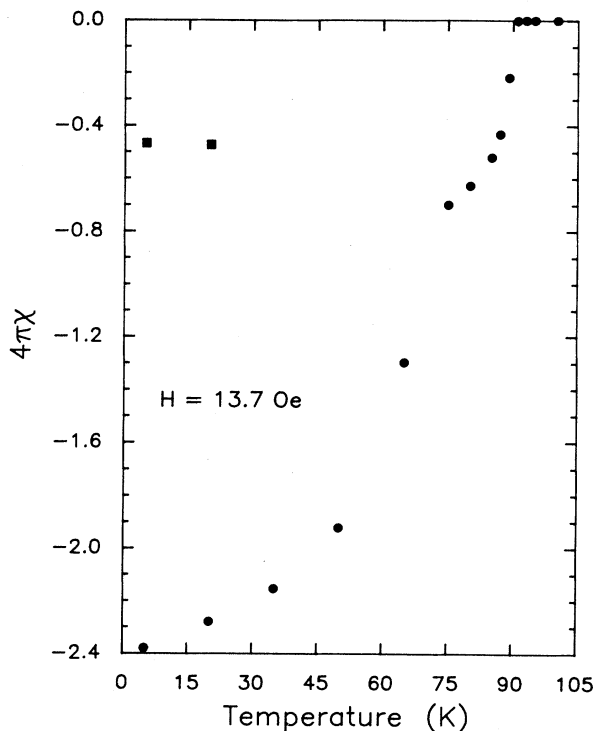


FIG. 1. The magnetic susceptibility (Gaussian units) of our sample in a 13.7-Oe field. The circles represent zero-field cooled data, while the field cooled data are plotted as squares.

To investigate the cause of this knee, we ground the sample and remeasured its susceptibility. The knee disappeared, and the sample showed the sharp transition seen in Fig. 2. We therefore attribute the knee seen in the pelleted sample's data to intergrain coupling, which causes flux to be excluded from the voids in the sample.

Junod *et al.*¹² measured the paramagnetic contribution of Cu^{2+} atoms in the magnetic susceptibility of $\text{YBa}_2\text{Cu}_3\text{O}_{7-x}$. They were able to correlate the size of this signal to the concentration of BaCuO_2 in samples with fairly high levels of this impurity. With this in mind, we measured the magnetic susceptibility of our sample at high temperatures and plotted χT versus T as in Fig. 3. (There is a possibility that iron atoms, coming from the starting materials, contributed to the susceptibility of the sample. Based on the assays of our prereacted powders, we placed an upper limit of 5 ppm iron atoms in the sample. We calculated the expected Curie-Weiss contribution from these iron atoms and found that it was insignificant.) The y intercept of the line yields the coefficient of the paramagnetic contribution, from which, assuming a moment of $1.5\mu_B$, we find that the ratio of the number of Cu^{2+} to the number of Cu atoms ($[\text{Cu}^{2+}]/[\text{Cu}]$ concentration) is 8.3%. This, in turn, corresponds to a concentration of 2.9 wt. % of BaCuO_2 . We have seen, however, from our x-ray data and our Raman data that there is less than 1% and 0.3%, respectively, of BaCuO_2 in our sample.

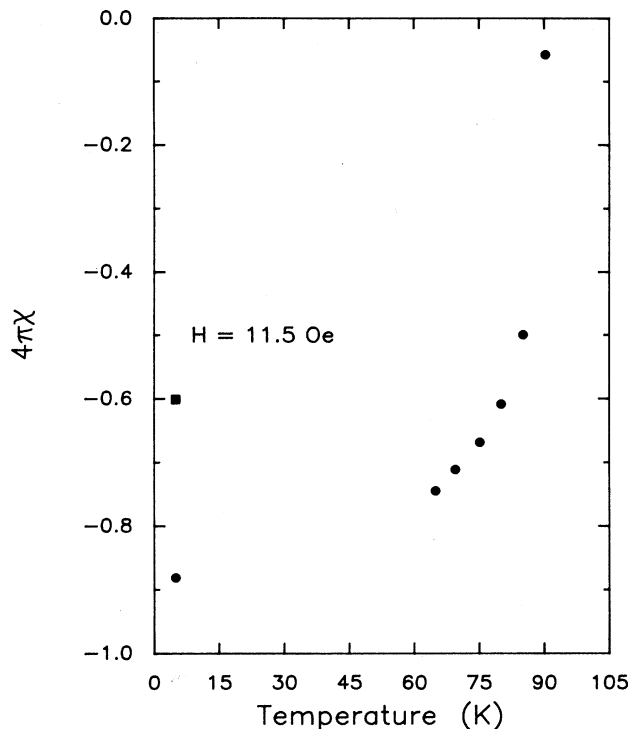


FIG. 2. The magnetic susceptibility (Gaussian units), of our sample after grinding it. The data were taken by cooling to 5 K in zero field (circles), setting the field to 11.5 Oe, and warming the sample above T_c . The solid square was taken after cooling to 5 K in the 11.5-Oe field.

One possible explanation for our high-temperature susceptibility data is that the paramagnetism arises from Cu^{2+} atoms that are in one of the other common impurity phases. Our measured Cu^{2+} ratio corresponds to 5.71 wt. % of Y_2BaCuO_5 (compared to 2 wt. % detected with x rays) or to 1 wt. % of CuO .

The spin susceptibility contribution from Cu^{2+} ions is thought to be intrinsic to a related compound, $\text{La}_{2-x}\text{Sr}_x\text{CuO}_{4-y}$ (Ref. 13), possibly because of missing oxygen atoms in the neighborhood of some of the copper atoms. That Cu^{2+} ions are also intrinsic to $\text{YBa}_2\text{Cu}_3\text{O}_{7-x}$ is not unlikely, and may affect the susceptibility of this compound in the normal state.

We were able to get a much better fit by assuming a constant term plus a Curie-Weiss type dependence with a Néel temperature of -39 K. In Fig. 3, we plot χ multiplied by $(T+39$ K) versus T to show the quality of this fit. Again, assuming a moment of $1.5\mu_B$, we calculate the number of magnetic atoms to be 0.123 per Cu atom. Since a Curie-Weiss dependence has not been seen in BaCuO_2 ,¹² we do not believe the high-temperature susceptibility indicates the presence of this impurity.

We also needed to determine whether the magnetic field would be distorted by the superconducting sample. We therefore measured the magnetic moment of the pelletized sample in fields of 1, 2, and 3 T. Before the measurement in each field, the sample was warmed above its

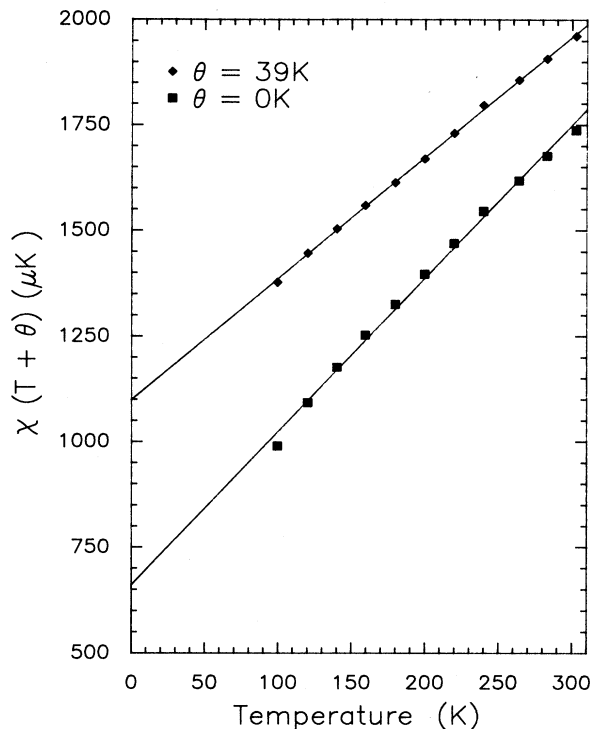


FIG. 3. The high-temperature magnetic susceptibility of our sample (Gaussian units), measured in a field of 1 kOe. The squares represent a Curie-law temperature dependence by plotting χT vs T ; the diamonds represent a Curie-Weiss dependence by plotting $\chi(T+39$ K). The Curie-Weiss law gives a better fit to the data.

superconducting transition and zero-field cooled to 2 K. The data shown in Fig. 4 are nearly temperature independent between 2 and 6 K in all fields except 1 T. The 1-T data vary linearly between 2 and 6 K and are reproducible from sample to sample, and though this effect appears to be dramatic in Fig. 4, it is really a small change in the flux penetrating the sample (from 92% at 2 K to 96% at 6 K). The fraction of the field penetrating the sample is given by the ratio

$$\frac{B}{H} = 1 + 4\pi\chi, \quad (1)$$

which, as shown in Table I, is close to unity. The magnetic field can therefore be assumed to be essentially undisturbed by the sample.

We need to know the approximate spacing between fluxoids so we can calculate the effect that the magnetic field has on the heat capacity. If we assume an equilateral triangular lattice of fluxoids, we can find the distance L between them by the formula

$$L = \left[\frac{2\Phi_0}{\sqrt{3}B} \right]^{1/2} \quad (2)$$

(Φ_0 is the flux quantum and B is the value of the field inside the superconductor.) The calculated spacing be-

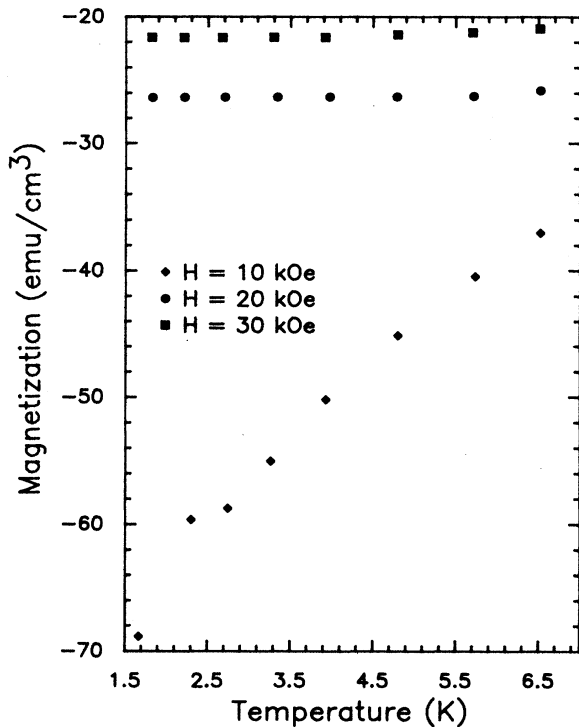


FIG. 4. The magnetization of our sample taken in high fields (Gaussian units). The sample was zero-field cooled and the data were taken while warming in the field. These data show that the shielding of the sample is negligible for fields ≥ 1 T.

tween fluxoids in each field is given in Table I. Our analysis of the specific heat data is unaffected by our assumption that the flux lattice is triangular.

C. Heat capacity

We measured the heat capacity of a 2.567-g sample of $\text{YBa}_2\text{Cu}_3\text{O}_{7-x}$ in fields of 0, 1, 2, and 3 T and in the temperature range from 2 to 10 K. The heat capacity was measured with an adiabatic, computer-controlled calorimeter, using the pulse method.¹⁴ When the sample had reached thermal equilibrium, we measured the temperature of the sample before and after applying a measured heat pulse. The heat was supplied by a current pulse passing through a 1000- Ω strain gauge, and the temperature was measured with a calibrated carbon-glass thermometer.¹⁵ [The results of Sample, Rubin, and Brant¹⁶ show that the field dependence of the calibration for a carbon-glass thermometer is very small ($< 1\%$ for fields below 3 T)]. The total energy supplied by the heater divided by the temperature rise is the heat capacity.

TABLE I. Magnetization data.

H (T)	χ (memu/Oe cm^3)	B/H	L (\AA)
1.0	-4.25	0.95	503
2.0	-1.34	0.98	349
3.0	-0.723	0.99	284

We started each temperature scan by closing a mechanical heat switch and cooling the sample to 4.2 K in zero field. With the heat switch still closed, we turned up the magnetic field and measured its value with a Hall effect probe.¹⁵ The sample warmed to approximately 6 K because of Joule heating from the eddy currents. After the field was fixed, we pumped on the helium bath to reduce the sample temperature to 1.5 K. We then slowly opened the heat switch and measured the sample's heat capacity while warming the sample from 2 to 10 K. After reaching 10 K, we warmed the sample above its superconducting transition, turned the magnetic field off, and closed the heat switch to cool the sample back down to 4.2 K.

We measured the heat capacity of the empty cell in magnetic fields so we could subtract from the data any effects of the magnetic field on the addenda, which were a thin copper stage, one carbon glass and one platinum thermometer, a heater, and a small, measured amount of vacuum grease used to stick the samples down. The heat capacity of the addenda was field dependent; at 3 T, the field-generated heat capacity of the addenda varied from 14% of the zero-field value at 2 K to 2.5% at 6 K. The ratio of the addenda's heat capacity to that of the sample was approximately 0.5.

We subtracted the field-dependent contribution of the addenda and divided the heat capacity by the number of moles in the sample, to obtain the specific heat, c (see Fig. 5). In order to see more clearly the temperature depen-

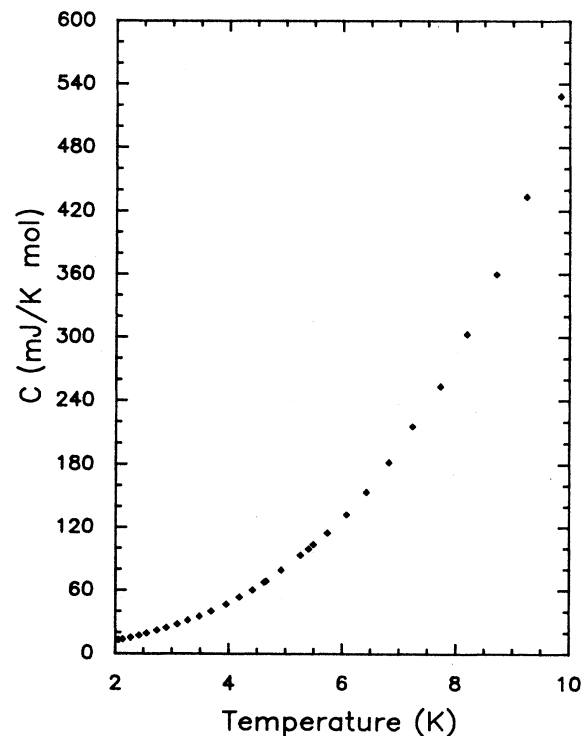


FIG. 5. The low-temperature specific heat of our sample taken in zero field. The 1-, 2-, and 3-T field data lie very close to the zero-field points and are omitted for clarity.

dence of the specific heat, we plotted c/T as a function of T^2 , as shown in Fig. 6.

The data plotted in Fig. 6 show linear behavior at temperatures below 7 K. The zero-field data begin to increase faster than linearly near $T=7.5$ K, indicating a deviation from Debye behavior. The in-field data curve upward from the straight line at a slightly lower temperature (approximately 6 K for the 3 T data). The c/T versus T^2 data are replotted in Fig. 7 to emphasize the linear behavior at low temperatures. The data in all three fields are linear below 6 K, and they show no evidence of an upturn as the temperature decreases. Such an upturn would have indicated magnetic impurities. Using a least-squares fit, we can extrapolate these data to $T=0$ to extract the coefficients of

$$c = \alpha(H)T + \beta(H)T^3. \quad (3)$$

Defining α_0 and β_0 to be the zero-field values, we rewrite Eq. (3),

$$c = [\alpha_0 + \alpha_1(H)]T + [\beta_0 + \beta_1(H)]T^3. \quad (4)$$

The measured values of α_0 and β_0 are 4.38 mJ/mol K² and 0.478 mJ/mol K⁴, respectively. The field-dependent coefficients are given in Table II and are plotted as a function of the applied field in Fig. 8.

We are not the first to report the field dependence of the specific heat of YBa₂Cu₃O_{7-x}. Phillips *et al.*¹⁷ and van der Meulen *et al.*¹⁸ measured the field dependence of the specific heat of samples for which c/T had significant

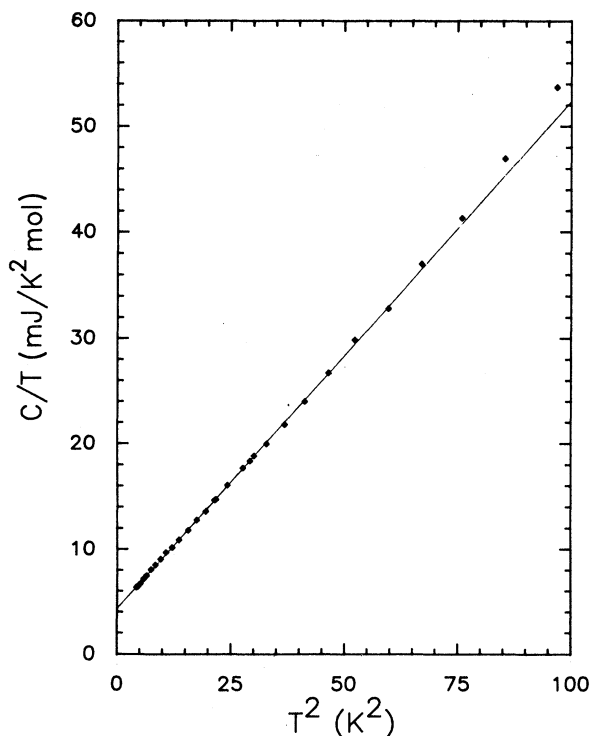


FIG. 6. The low-temperature, zero-field specific heat of our sample plotted as c/T vs T^2 .

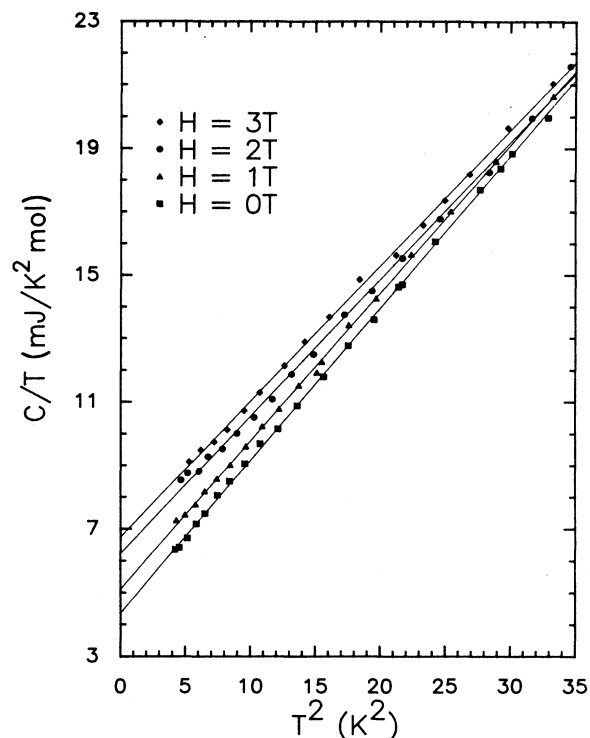


FIG. 7. The low-temperature specific heat of our sample, emphasizing the behavior as T approaches zero. The data are taken in fields of 0, 1, 2, and 3 T, and the values of the coefficients of the linear and cubic terms are clearly varying with field.

upturns in zero field at low temperatures. The in-field data exhibited Schottky anomalies correlated with these upturns. The presence of such a feature in the specific heat probably indicates the existence of impurity phases, which are apparently absent from our samples. Caspary *et al.*¹⁹ measured the specific heat in fields of 0 and 8 T and in the temperature range from 0.08 to 2 K. They saw an upturn only at the lowest temperatures, and they saw a term in the specific heat linear in T ; it became vanishingly small in the 8-T field. They attributed the temperature and field dependence of their data to spin glass behavior of the Cu²⁺ ions. Sasaki *et al.*²⁰ measured the specific heat in 0-, 1-, and 3-T fields. Their data showed a small, low-temperature upturn that increased with field. They held the cubic term fixed and fitted the data to a function of the form

$$c = a/T^2 + \alpha T + \beta T^3 + gT^5. \quad (5)$$

Their coefficients for the linear term were 5.1, 5.8, and 6.7 mJ/mol K² in fields of 0, 1, and 3 T, respectively. (This compares to our measured values of 4.37, 5.11, and 6.74 mJ/mol K² in these same fields.) Forgan *et al.*²¹ have also measured the magnetic field dependence of the linear term in the specific heat of YBa₂Cu₃O_{7-x}. They find a linear term which is about twice as large as ours when no magnetic field is applied, and a field dependence of the linear term which is approximately half as large as

TABLE II. Specific heat data. The definitions of $\alpha_1(H)$ and $\beta_1(H)$ are given in Eq. (4).

H (T)	$\alpha_1(H)$ (mJ/mol K ²)	$\beta_1(H)$ (mJ/mol K ⁴)	Δs (mJ/mol K)	Θ_D (K)
0.0	0.0	0.0	0.0	375
1.0	0.74	-0.011	3.58	378
2.0	1.99	-0.049	7.69	389
3.0	2.37	-0.051	10.55	390

we find. The analysis of their data is, however, complicated by an upturn in the c/T versus T^2 curve, starting about 10 K. Such an upturn makes it very difficult to extract the linear term, since this term is dependent on the way the upturn is modeled.

Finally, Baak *et al.*²² measured the specific heat of a mosaic of 80 single crystals and found no evidence of a linear term. Rather, they fitted their data to a function,

$$c = AT^{0.42} + BT^3, \quad (6)$$

over the entire temperature range, 0.4–30 K. Baak *et al.* did not plot c/T versus T^2 , nor did they plot the temperature dependence of their data on a linear scale; unlike Baak *et al.*, we did not see a purely cubic temperature dependence above 7 K. In contrast, von Molnar *et al.*²³ measured the low-temperature specific heat of a mosaic of single crystals and did not see a fractional power dependence of c on T at low temperatures.

Summing up, several authors have measured the field dependence of the low-temperature specific heat and have gotten a variety of results. Our measurements do not agree with other results reported in the literature, em-

phasizing the importance of making more measurements of the field-dependent specific heat of $\text{YBa}_2\text{Cu}_3\text{O}_{7-x}$.

We can now calculate several material parameters. The Debye temperature, calculated from²⁴

$$\Theta_D = \left[\frac{12\pi^4 nk_B}{5 \beta_0} \right]^{1/3}, \quad (7)$$

where n is the number of atoms per mole, is 375 K in zero field. We can also determine whether the linear dependence on temperature below 7 K is intrinsic or due to BaCuO_2 impurities. Using the data of Kuentzler *et al.*,⁷ we calculate that an impurity level of 1% by weight of BaCuO_2 would be necessary to explain the linear term. The Raman data showed that there is less than 0.3% of this impurity, so that BaCuO_2 impurities cannot account for the size of the linear term seen by us in zero field at low temperature.

Eckert *et al.* have correlated the number of Cu^{2+} atoms (and possibly the concentration of BaCuO_2 impurities) present in a sample with the size of the linear term in the low-temperature heat capacity.⁹ Using the ratio of $[\text{Cu}^{2+}]/[\text{Cu}]$ concentration that we get from fitting a Curie law to our susceptibility data, we estimate that the coefficient of the linear term in the heat capacity would be 17.7 mJ/mol K². This is about four times higher than what we measure, suggesting that Eckert's correlation between the linear term in the heat capacity and the size of the paramagnetic contribution to $\chi(T)$ does not hold for our samples.

We do not believe that our samples are contaminated with BaCuO_2 because we do not see an upturn in the low-temperature heat capacity measured in field. Under the assumption that any Cu^{2+} atoms located in an impurity phase would have their orbital moments quenched, these Cu^{2+} ions would have two energy levels in a magnetic field, and their heat capacity would exhibit a Schottky anomaly.²⁵ This anomaly was seen in the field-dependent specific heat of BaCuO_2 , measured by Arhens *et al.*²⁶

We therefore believe the field-dependent coefficients of Table I represent intrinsic parameters of $\text{YBa}_2\text{Cu}_3\text{O}_{7-x}$. The assertion that the linear term in the low-temperature specific heat is intrinsic is further supported by other specific heat data,²⁷ as well as by the Raman data of Slakey *et al.*²⁸ Their data suggest the existence of a low-energy continuum of electronic states well below T_c .

The field-generated contribution to the heat capacity arises because the magnetic field increases the entropy of the sample, which we calculate by integrating c/T . At the superconducting transition, there is a field-dependent decrease in the entropy;^{29,30} we want to find out how

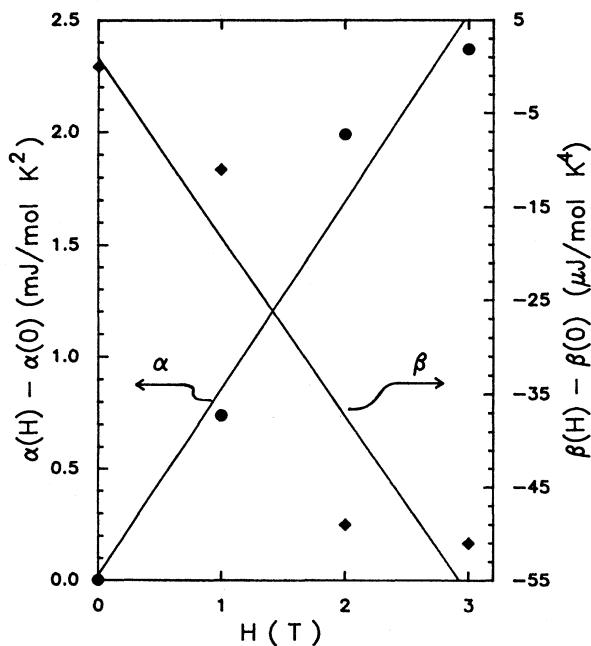


FIG. 8. The values of the coefficients of the linear (circles) and cubic (diamonds) terms. The zero-field contribution is subtracted and the data are plotted as a function of field. The lines represent linear least-squares fits to the points.

much of this entropy "shows up" at low temperatures. If we assume that c/T versus T^2 is linear from $T=0$ to 6 K, the field-dependent molar entropy change Δs can be calculated from

$$\Delta s = \alpha_1 T + \frac{1}{3} \beta_1 T^3. \quad (8)$$

The values for the excess entropy up to 6 K are given in Table II. The field-dependent decrease in the entropy at the superconducting transition can be found from Fig. 2 of Salamon *et al.*²⁹ Estimating

$$\Delta s(T_c, 3T) = 71.3 \text{ mJ/K mol},$$

the entropy change seen in the low-temperature data accounts only for only 15% of this.

III. CALCULATION

We have seen field-induced changes in both the linear and cubic terms of the low-temperature heat capacity. These have been predicted theoretically by Maki⁵ and by Fetter and Hohenberg⁶ by analyzing the free energy of the superconducting electrons in a magnetic field. The London model ($\xi \ll \lambda$) is assumed. For $\text{YBa}_2\text{Cu}_3\text{O}_{7-x}$, $\xi \approx 10 \text{ \AA}$, and $\lambda \approx 1200 \text{ \AA}$. When the field is turned on, the free energy is increased by

$$\mathcal{F} = \frac{1}{8\pi} \int [h^2 + \lambda^2 (\nabla \times h)^2] d^3x; \quad (9)$$

$\lambda^2 (\nabla \times h)^2$ is the kinetic energy density and h is the local magnetic field, the spatial average of which is B . From this, they calculate the Gibbs free energy difference,

$$\Delta G = \mathcal{F} - \frac{BH}{4\pi}. \quad (10)$$

The difference in entropy is calculated,

$$\Delta s = - \left[\frac{\partial \Delta G}{\partial T} \right]_H. \quad (11)$$

This expression ignores the contribution to the entropy made by the electrons in the normal cores. Using a Sommerfeld constant of $3 \times 10^3 \text{ erg/cm}^3 \text{ K}^2$, we find the contribution of the normal electrons is 2% of the measured entropy change in field, so ignoring the normal-core contribution to the entropy is justified. Finally, the specific heat enhancement caused by the magnetic field can be found from the derivative of the entropy difference,

$$\Delta c = T \left[\frac{\partial \Delta s}{\partial T} \right]_H. \quad (12)$$

Maki calculated the change in the heat capacity of a superconductor in a magnetic field, by assuming the superconductor is in the dirty limit (the mean free path l is much smaller than the coherence length ξ).⁵ Since the coherence length of $\text{YBa}_2\text{Cu}_3\text{O}_{7-x}$ is extremely small, these materials cannot be in the dirty limit. Nevertheless, we calculated the expected enhancements from Maki's theory and found that $\alpha_1/B = 6.90 \times 10^{-3} \text{ erg/K}^2 \text{ cm}^3 \text{ G}$ and $\beta_1 = 0.114 \text{ erg/K}^4 \text{ cm}^3$ at 20 kG. We measure

$\alpha_1/B = 7.96 \times 10^{-3} \text{ erg/K}^2 \text{ cm}^3 \text{ G}$ and $\beta_1 = -4.70 \text{ erg/K}^4 \text{ cm}^3$ at 20 kG. The change in the coefficient of the cubic terms agrees neither in sign nor in magnitude with the calculated value. The field-dependent enhancement of the linear term's coefficient is quite close to the value predicted by Maki. This is probably a coincidence, because the ratio of l to ξ shows $\text{YBa}_2\text{Cu}_3\text{O}_{7-x}$ to be in the clean rather than the dirty limit.

We next compare our data to the conclusions of Fetter and Hohenberg.⁶ Using the preceding analysis and assuming the clean limit, their Eq. (E10) gives the following expression for the heat capacity difference Δc ,

$$\Delta c = - \frac{TB}{4\pi} \frac{d^2 H_{c1}}{dT^2} + \frac{T}{4\pi} \left[\frac{dH_{c1}}{dT} \right]^2 + \dots \quad (13)$$

Combining these equations with⁶

$$H_{c1} = \sqrt{2} H_c(t) \frac{\ln \kappa_3(t)}{2\kappa_3(t)} \quad (14)$$

and

$$\kappa_3(t) = \sqrt{2} \left[\frac{2e}{\hbar} \right] H_c(t) \lambda^2(t), \quad (15)$$

and using²⁷

$$H_c(t) \propto 1 - t^2 \quad (16)$$

and

$$\lambda^2 \propto (1 - t^4)^{-1}, \quad (17)$$

we find that

$$\alpha_1 = \frac{\Phi_0}{8\pi^2 \lambda^2 T_c^2} B \quad (18a)$$

and

$$\beta_1 = \frac{\Phi_0}{8\pi^2 \lambda^2 T_c^4} \left[3B + \frac{\Phi_0}{2\pi \lambda^2} \right]. \quad (18b)$$

These two expressions are inconsistent with our data. From Eqs. (18a) and (18b), α_1/β_1 is of order $T_c^2 \approx 10^4 \text{ K}^2$; this is not seen in our data. If we solve Eq. (18a) for λ and replace α_1 by its measured value, we find that λ must be 638 \AA . As the measured values published for the penetration depth range from 900 to 1400 \AA ,³¹⁻³³ it is unlikely that these theoretical expressions correspond to our data.

The problem with this analysis may be that it assumes the superconductor is isotropic. This is unlikely, as workers have seen large anisotropies in the upper and lower critical fields of the $\text{YBa}_2\text{Cu}_3\text{O}_{7-x}$ superconductors.^{31,33,34}

Kogan and his collaborators^{35,36} have investigated the effect of including anisotropy in the effective mass tensor on the Helmholtz free energy of a superconductor. They find that the field-dependent free energy term calculated in the London limit ($\xi \ll \lambda$) is replaced by one of the form³⁵

$$\mathcal{F} = \frac{1}{8\pi} \int [h^2 + \lambda^2 m_{ij} (\nabla \times h)_i (\nabla \times h)_j] d^3x. \quad (19)$$

(m_{ij} is a component of the reduced effective mass tensor and λ is the mean square of the penetration depth averaged over the principal directions of the crystal.) Later, we will introduce the variables $m_{1,2,3}$, the diagonal elements of the effective mass tensor corresponding to the a, b, c crystal directions, respectively. We will find that the term $\lambda^2 m_{ij} (\nabla \times h)_i (\nabla \times h)_j$, the kinetic energy density, is responsible for a field-induced change of the linear term in $c(T)$. If we assume uniaxial symmetry, $m_1 = m_2$, Eq. (19) can be expanded to second order in L/λ to yield³⁶

$$8\pi\mathcal{F} = B^2 + B^2 \frac{m_{zz}}{m_1} \frac{L^2}{\lambda^2} \sum' (m_{zz}g_x^2 + m_3g_y^2)^{-1}, \quad (20)$$

with

$$m_{zz} = m_1 \sin^2\theta + m_3 \cos^2\theta.$$

(g_i is a dimensionless reciprocal-lattice vector; $g_i = \sqrt{\Phi_0/B} G_i$, where G_i is a reciprocal-lattice vector of the fluxoid array.) The sum is carried out over nonzero vectors of the reciprocal flux lattice. The three components of the magnetic field can be found by differentiating the expression for the free energy,

$$H_i = \frac{\partial}{\partial B_i} \left[B^2 + B^2 \frac{m_{zz}}{m_1} \frac{L^2}{\lambda^2} \sum' (m_{zz}g_x^2 + m_3g_y^2)^{-1} \right]. \quad (21)$$

In order to evaluate this derivative, we need to know dL^2/dB . For a periodic array of fluxoids, each carrying one flux quantum Φ_0 ,

$$L^2 = \text{const} \times \frac{\Phi_0}{B}. \quad (22)$$

Therefore,

$$\frac{\partial L^2}{\partial B} = -\text{const} \times \frac{\Phi_0}{B^2} = -\frac{L^2}{B}. \quad (23)$$

If we evaluate the derivative of \mathcal{F} with respect to B and define

$$\delta_r = (m_{zz}g_x^2 + m_3g_y^2), \quad (24)$$

then

$$\begin{aligned} \mathbf{H} &= \mathbf{B} \left[1 + \frac{m_{zz}}{m_1} \frac{L^2}{\lambda^2} \sum_r' \delta_r^{-1} \right] - \frac{\mathbf{B}}{2} \left[\frac{L^2}{\lambda^2} \frac{m_{zz}}{m_1} \sum_r' \delta_r^{-1} \right] \\ &= \mathbf{B} \left[1 + \frac{1}{2} \frac{m_{zz}}{m_1} \frac{L^2}{\lambda^2} \sum_r' \delta_r^{-1} \right]. \end{aligned} \quad (25)$$

Substituting into Eqs. (10)–(12), we find

$$\Delta c = \frac{T}{4\pi} \left[\left(\frac{\partial B}{\partial T} \right)^2 + B \frac{\partial^2 B}{\partial T^2} \right]. \quad (26)$$

The partial derivative of B with respect to T can be found if we use the condition

$$\frac{\partial H}{\partial T} = 0.$$

Cambell, Doria, and Kogan³⁶ have already found the relationship between H and B ,

$$H_z = B_z \left[1 + \frac{1}{8\pi} \frac{\Phi_0 m_3}{\lambda^2 B \sqrt{m_{zz}}} \ln \left[\frac{\eta H_{c2}}{B} \right] \right], \quad (27a)$$

and

$$H_x = B_x \left[1 + \frac{1}{8\pi} \frac{\Phi_0 m_i}{\lambda^2 B \sqrt{m_{zz}}} \ln \left[\frac{\eta H_{c2}}{B} \right] \right]. \quad (27b)$$

[η , defined as β in Eq. (3.64) of de Gennes,³⁷ is a geometrical factor of order unity that depends on the shape of the unit cell of the flux-lattice.] The second term in each of these expressions is of order H_{c1}/B . Since this ratio is much smaller than unity, we want to find the value of the magnitude of H only to first order in this term. Therefore, using $B_x = B \sin\theta$ and $B_z = B \cos\theta$, we find

$$\begin{aligned} H^2 &= B^2 + 2B^2 \left[\frac{m_1 \sin^2(\theta) + m_3 \cos^2(\theta)}{B \sqrt{m_{zz}}} \right] \\ &\quad \times \frac{\Phi_0}{8\pi \lambda^2} \ln \left[\frac{\eta H_{c2}}{B} \right]. \end{aligned} \quad (28)$$

Substituting $m_1 \sin^2\theta + m_3 \cos^2\theta$ for m_{zz} ,

$$H = B \left[1 + \frac{2\sqrt{m_{zz}} \Phi_0}{8\pi B \lambda^2} \ln \left[\frac{\eta H_{c2}}{B} \right] \right]^{1/2}. \quad (29)$$

Expanding the square root to first order in H_{c1}/B and defining

$$\Gamma = \frac{\sqrt{m_{zz}} \Phi_0}{8\pi}, \quad (30)$$

we have

$$H = B + \Gamma \lambda^{-2} \ln \left[\frac{\eta H_{c2}}{B} \right]. \quad (31)$$

Hence,

$$\begin{aligned} 0 = \frac{\partial H}{\partial T} &= \frac{\partial B}{\partial T} + \Gamma \frac{\partial \lambda^{-2}}{\partial T} \ln \left[\frac{\eta H_{c2}}{B} \right] \\ &\quad + \Gamma \lambda^{-2} \left[\frac{1}{H_{c2}} \frac{\partial H_{c2}}{\partial T} - \frac{1}{B} \frac{\partial B}{\partial T} \right]. \end{aligned} \quad (32)$$

Combining terms,

$$\begin{aligned} -\frac{\partial B}{\partial T} \left[1 - \Gamma \frac{\lambda^{-2}}{B} \right] &= \Gamma \left[\frac{\partial \lambda^{-2}}{\partial T} \ln \left[\frac{\eta H_{c2}}{B} \right] \right. \\ &\quad \left. + \frac{\lambda^{-2}}{H_{c2}} \frac{\partial H_{c2}}{\partial T} \right]. \end{aligned} \quad (33)$$

The second term on the left-hand side is of order

$H_{c1}/B \ll 1$. The derivative of B with respect to T is therefore

$$\frac{\partial B}{\partial T} = -\Gamma \left[\frac{\partial \lambda^{-2}}{\partial T} \ln \left(\frac{\eta H_{c2}}{B} \right) + \frac{\lambda^{-2}}{H_{c2}} \frac{\partial H_{c2}}{\partial T} \right]. \quad (34)$$

Using the first and second derivatives of λ^{-2} and H_{c2}

with respect to temperature, calculated in the Appendix, we find

$$\left[\frac{\partial B}{\partial T} \right]^2 = \Gamma^2 \frac{4a^2}{\lambda^4(0)T_c^4} T^2 \quad (35)$$

to second order in t ($t \equiv T/T_c$). Taking the second derivative of B with respect to T ,

$$\begin{aligned} -\frac{1}{\Gamma} \frac{\partial^2 B}{\partial T^2} &= \frac{\partial \lambda^{-2}(T)}{\partial T} \left[\frac{1}{H_{c2}(T)} \frac{\partial H_{c2}(T)}{\partial T} - \frac{1}{B} \frac{\partial B}{\partial T} \right] + \frac{\partial^2 \lambda^{-2}(T)}{\partial T^2} \ln \left(\frac{\eta H_{c2}}{B} \right) + \frac{\partial \lambda^{-2}(T)}{\partial T} \frac{1}{H_{c2}(T)} \frac{\partial H_{c2}(T)}{\partial T} \\ &\quad - \lambda^{-2}(T) \left[\frac{1}{H_{c2}(T)} \frac{\partial H_{c2}}{\partial T} \right]^2 + \frac{\lambda^{-2}(T)}{H_{c2}(T)} \frac{\partial^2 H_{c2}(T)}{\partial T^2}. \end{aligned} \quad (36)$$

Keeping terms of order t^2 , we have

$$-\frac{1}{\Gamma} \frac{d^2 B}{dT^2} = \frac{d^2 \lambda^{-2}(T)}{dT^2} \ln \left(\frac{\eta H_{c2}}{B} \right) - \lambda^{-2}(T) \left[\frac{1}{H_{c2}(T)} \frac{dH_{c2}}{dT} \right]^2 + \frac{\lambda^{-2}(T)}{H_{c2}(T)} \frac{d^2 H_{c2}(T)}{dT^2}. \quad (37)$$

Substituting values from the Appendix and defining ξ ,

$$\xi = 2 \ln \left[\frac{\eta H_{c2}}{B} \right], \quad (38)$$

$$-\frac{1}{\Gamma} \frac{d^2 B}{dT^2} = -\frac{12t^2}{\lambda^2(0)T_c^2} \frac{\xi}{2} - \frac{1}{\lambda^2(0)} \left[\frac{-2atH_{c2}(0)}{T_c H_{c2}(0)(1-at^2)} \right]^2 + \frac{1}{\lambda^2(0)T_c^2} \left[\frac{H_{c2}(0)(-2a+12dt^2)}{H_{c2}(0)(1-at^2)} \right]. \quad (39)$$

Expanding and keeping terms up to order t^2 ,

$$\begin{aligned} -\frac{1}{\Gamma} \frac{d^2 B}{dT^2} &= -\frac{12t^2}{\lambda^2(0)T_c^2} \frac{\xi}{2} - \frac{4a^2 t^2}{\lambda^2(0)T_c^2} + \frac{-2a + (12d - 2a^2)t^2}{\lambda^2(0)T_c^2} \\ &= \frac{2}{\lambda^2(0)T_c^2} [-a + 3(-\xi - a^2 + 2d)t^2]. \end{aligned} \quad (40)$$

Substituting the first and second derivatives of B with respect to T into Eq. (26) to find Δc ,

$$\begin{aligned} \frac{4\pi}{T} \Delta c &= \Gamma^2 \frac{4a^2}{\lambda^4(0)T_c^4} t^2 - B \Gamma \frac{2}{\lambda^2(0)T_c^2} [-a + 3(-\xi - a^2 + 2d)t^2] \\ &= \Gamma \frac{2B}{\lambda^2(0)T_c^2} \left[a - 3 \left[-\xi - a^2 + 2d - \Gamma \frac{2a^2}{3B\lambda^2(0)} \right] t^2 \right]. \end{aligned} \quad (41)$$

The last term in the parentheses is of order $a^2 H_{c1}/B$ and may be neglected compared to the second term. Substituting for ξ and Γ and rewriting Δc as in Eqs. (18a) and (18b),

$$\alpha_1 = \frac{\sqrt{m_{zz}} \Phi_0}{8\pi} \frac{2aB}{4\pi\lambda^2(0)T_c^2} \quad (42a)$$

and

$$\beta_1 = \frac{\sqrt{m_{zz}} \Phi_0}{8\pi} \frac{6B}{4\pi\lambda^2(0)T_c^4} \left[2 \ln \left[\frac{\eta H_{c2}}{B} \right] + a^2 - 2d \right]. \quad (42b)$$

IV. DISCUSSION

We compare the results to our data for polycrystalline samples by averaging Eq. (42a) over a spherical shell, obtaining

$$\begin{aligned} \bar{\alpha}_1 &= \frac{\Phi_0}{8\pi} \frac{aB}{4\pi\lambda^2(0)T_c^2} \\ &\quad \times \int_{-1}^1 d(\cos\theta) \left[m_1 \left[\sin^2\theta + \frac{m_3}{m_1} \cos^2\theta \right] \right]^{1/2}. \end{aligned} \quad (43)$$

The anisotropy factor γ is defined by

$$\gamma = \sqrt{m_3/m_1}, \quad (44)$$

where m_1 , m_2 , and m_3 are the diagonal elements of the effective mass tensor corresponding to the a , b , and c crystal directions, respectively. Rewriting Eq. (43),

$$\frac{\bar{\alpha}_1}{B} = \frac{a\Phi_0}{32\pi^2\lambda^2T_c^2\gamma^{1/3}} \int_{-1}^1 du [1 + (\gamma^2 - 1)u^2]^{1/2}. \quad (45)$$

The solution is³⁸

$$\frac{\bar{\alpha}_1}{B} = \frac{\Phi_0 a}{32\pi^2\lambda^2T_c^2\gamma^{1/3}} \times \left[\gamma + \frac{1}{2(\gamma^2 - 1)^{1/2}} \ln \left[\frac{\gamma + (\gamma^2 - 1)^{1/2}}{\gamma - (\gamma^2 - 1)^{1/2}} \right] \right]. \quad (46)$$

The experimentally measured value of $\bar{\alpha}_1/B$ can be found by fitting the data of Fig. 8 to a straight line. We scale the linear coefficients by the density, 6.38 g/cm³, and the atomic weight to find

$$\bar{\alpha}_1/B = 7.96 \times 10^{-3} \text{ erg/G K}^2 \text{ cm}^3. \quad (47)$$

We put this value into Eq. (46) and solve for the penetration depth, $\lambda\sqrt{m_1}$, with the magnetic field pointing in the c direction, as a function of the square root of the effective mass ratio (see Fig. 9). The anisotropy factor can be calculated from the ratio of dH_{c2}/dT parallel to the c axis to that perpendicular to the c axis,³² the measured values of which vary from 4 (Ref. 33) to 10 (Ref. 34). Using the Sommerfeld constant γ , Bardeen *et al.*

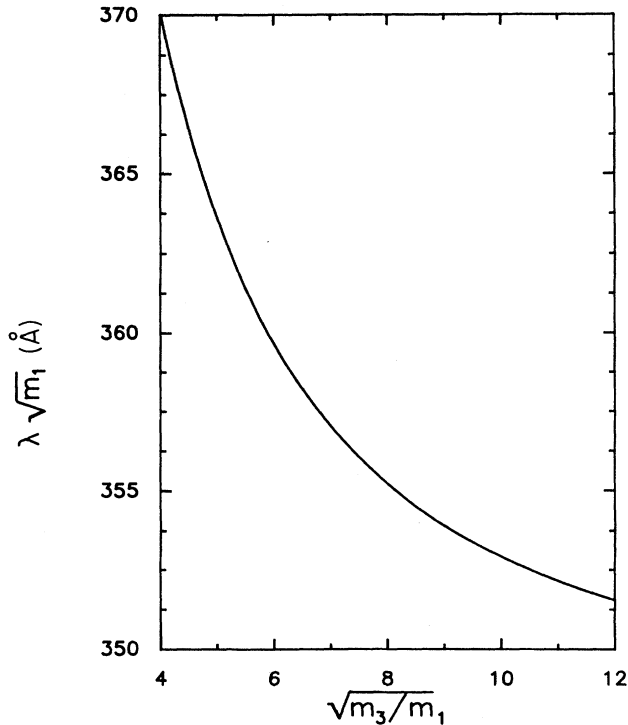


FIG. 9. The penetration depth [defined in Eq. (19)] as a function of the square root of the effective mass ratio, $\sqrt{m_3/m_1} = \gamma$. This curve is calculated using the value of the enhancement of the linear term with field as a parameter.

have calculated a value of 9 for the square root of the effective mass ratio, $\sqrt{m_3/m_1}$.³⁹ Our values for $\lambda\sqrt{m_1}$ plotted in Fig. 9 vary from 370 to 353 Å for γ ranging from 4 to 10. These penetration depths are lower than the measured values.³¹⁻³³ Farrell *et al.*⁴⁰ measured the intrinsic transverse magnetization for $\text{YBa}_2\text{Cu}_3\text{O}_{7-x}$ in a magnetic field. From this measurement, they determined γ to be 5.1, corresponding to a penetration depth with the field parallel to the crystal's c axis of 363 Å. This is outside of the range of the measured values of λ , 900-1400 Å.³¹⁻³³

To check the agreement between the calculated and measured values of β , we look at the ratio α_1/β_1 . We calculate the ratio of the theoretical values using Eqs. (42a) and (42b) and compare to the experimental data,

$$\frac{\alpha_1}{\beta_1} = \frac{aT_c^2}{3[2 \ln(\eta H_{c2}/B) + a^2 - 2d]}. \quad (48)$$

H_{c2} has not been measured, but is thought to be extremely large. To obtain a lower bound on α_1/β_1 , we assume that

$$\frac{H_{c2}}{B} = \frac{1000 \text{ T}}{1 \text{ T}}.$$

The value of the lower bound on α_1/β_1 is then 250 K². From our data, the measured value of this ratio is -43.7 K²; it has the wrong sign and is too small in magnitude. This probably means that the calculation does not account for all the mechanisms that contribute to β_1 .

Could the decrease in the cubic term with increasing field be explained as arising from a change in the phonon spectrum? Zhao and Ketterson⁴¹ have measured the sound velocity as a function of magnetic field at 4.2 K in sinter forged samples of $\text{YBa}_2\text{Cu}_3\text{O}_{7-x}$. They see no change in the sound velocity between 0 and 8 T to a sensitivity of 0.074%. The Debye temperature is directly proportional to the sound velocity,²⁴ so it should change by less than 0.028% between 0 and 3 T. We see much larger changes than this in the heat capacity data (see Table II), however, so we conclude that the decrease in the coefficient of the cubic term with field may not come from shifts in the phonon spectrum.

V. CONCLUSIONS

We have measured the heat capacity of $\text{YBa}_2\text{Cu}_3\text{O}_{7-x}$ as a function of temperature and magnetic field. Below 10 K, we see a linear plus cubic temperature dependence that varies with field. Based on our correlations with x-ray, Raman, and magnetic susceptibility data, all measured on the same sample, we believe that the linear term is intrinsic to this material.

Much of the low-temperature heat capacity data reported in the literature exhibits an upturn below 4 K. Our data show no evidence of an upturn in zero field or in magnetic fields up to 3 T. This indicates that our samples are free of paramagnetic impurities. Specifically, we believe our samples are nearly free of BaCuO_2 . Our heat capacity data exhibit a different field dependence than the data reported in the literature by other groups; further-

more, the results of these other groups differ from each other. We believe this is due to variations in the amount of BaCuO₂ impurity in the samples of the various groups.

The field dependence of the linear term in our heat capacity data can be interpreted by using Ginzburg-Landau theory. We calculate the expected enhancement for a strongly type II (London limit), anisotropic superconductor. We are able to get good agreement between our measured coefficient of the linear term and our calculation if we assume that the square root of the effective mass ratio, $(m_3/m_1)^{1/2}$, is 5.1, and the London penetration depth, with the field parallel to the *c* axis, is 363 Å. This value of the penetration depth is, however, smaller than the measured values, so the Ginzburg-Landau theory is apparently unable to explain the magnetic-field-induced enhancement of the heat capacity of YBa₂Cu₃O_{7-x}. The measured field dependence of the specific heat is larger than that indicated by theory for accepted values of the London penetration depth. Irreversibility effects, including flux pinning, cannot be responsible for this difficulty, since they would cause a discrepancy of the opposite sign. We note that the theory, as applied here, does not take account of the layered structure of the compound or a possible field dependence of the coupling between the layers.

We do not understand why the cubic term decreases with increasing field. A change of this magnitude is inconsistent with measurements of the field dependence of the sound velocity and is not predicted by the enhancement calculated from Ginzburg-Landau theory. Perhaps the reason that the Ginzburg-Landau theory fails to account for our data is that the superconducting order parameter does not change slowly over a length characteristic of the atomic structure of these materials.

ACKNOWLEDGMENTS

This research was supported in part by National Science Foundation under Grant Nos. DMR 86-12860 (M.E.R., S.E.S., and D.M.G.), DMR 87-14555 (T.A.F. and D.M.G.), and DMR 87-15103 (F.S. and M.V.K.). Our x-ray diffraction measurements were made in the Center for Microanalysis of the Materials Research Laboratory. We thank Z. Zhao and J. B. Ketterson for providing us with their data prior to publication. We thank G. Eliashberg for helpful comments. We also thank our colleagues Joseph P. Rice, John Giapintzakis, and Edward D. Bukowski for their useful discussions and assistance with these experiments.

APPENDIX

In this appendix, we calculate the first two derivatives with respect to temperature of the upper critical field and the penetration depth. According to Mühlischlegel,⁴² as *T* approaches zero, the value for $[\lambda^2 - \lambda^2(0)]$ predicted by BCS theory should be proportional to $\exp(-\Delta/kT)$. Therefore, the first two derivatives of λ^2 vanish for $T \ll T_c$. Also, the dependence on temperature of the critical field, $H_c(T)$, is nearly equal to the two fluid model expression,⁴²

$$H_c(t) = H_c(0)(1-t^2). \quad (\text{A1a})$$

The temperature dependence of the penetration depth in the two-fluid model is given:³⁰

$$\lambda^{-2}(t) = \lambda^{-2}(0)(1-t^4), \quad (\text{A1b})$$

where

$$t \equiv \frac{T}{T_c}. \quad (\text{A1c})$$

The values of λ^{-2} and its first two derivatives are given to order t^2 by

$$\lambda^{-2} \approx \lambda^{-2}(0), \quad (\text{A2a})$$

$$\frac{\partial \lambda^{-2}(t)}{\partial T} \approx 0, \quad (\text{A2b})$$

$$\frac{\partial^2 \lambda^{-2}(t)}{\partial T^2} \approx -\frac{12\lambda^{-2}(0)}{T_c^2} t^2. \quad (\text{A2c})$$

The temperature dependence of H_{c2} has been calculated⁴³ in the clean limit for $T \ll T_c$.

$$H_{c2}(t) = 1.77\kappa H_c(t)(1+bt^2+ct^4),$$

$$H_{c2}(t) = 1.77\kappa H_c(0)(1-t^2)(1+bt^2+ct^4), \quad (\text{A3})$$

$$H_{c2}(t) = H_{c2}(0)[1+(b-1)t^2+(c-b)t^4].$$

($b = -0.43/1.77$ and $c = 0.07/1.77$.)⁴³ Let $a = 1-b$ and $d = c-b$. Then, $a = 1.24$ and $d = 0.282$. Rewriting H_{c2} and its derivatives to second order in *t*,

$$H_{c2}(t) \approx H_{c2}(0)(1-at^2), \quad (\text{A4a})$$

$$\frac{\partial H_{c2}(t)}{\partial T} \approx -\frac{H_{c2}(0)}{T_c} 2at, \quad (\text{A4b})$$

$$\frac{\partial^2 H_{c2}(t)}{\partial T^2} \approx \frac{H_{c2}(0)}{T_c^2} (-2a + 12dt^2). \quad (\text{A4c})$$

¹M. K. Wu, J. R. Ashburn, C. J. Torng, P. H. Hor, R. L. Meng, L. Gao, Z. J. Huang, Y. Q. Wang, and C. W. Chu, Phys. Rev. Lett. **58**, 908 (1987).

²D. M. Ginsberg, in *The Physical Properties of High Temperature Superconductors*, edited by D. M. Ginsberg (World Scientific, Singapore, 1989), Chap. 1.

³M. E. Reeves, T. A. Friedmann, and D. M. Ginsberg, Phys.

Rev. B **35**, 7207 (1988); B. D. Dunlap, M. V. Nevitt, M. Slaski, T. E. Klippert, Z. Sungaili, A. G. McKale, D. W. Capone II, R. B. Poeppel, and B. K. Flandermeyer, *ibid.* **35**, 7210 (1987); L. E. Wenger, J. T. Chen, G. W. Hunter, and E. M. Logothetis, *ibid.* **35**, 7213 (1987).

⁴R. A. Fisher, J. E. Gordon, and N. E. Phillips, J. Superconductivity **1**, 231 (1988).

- ⁵K. Maki, *Phys. Rev.* **139**, A702 (1965).
- ⁶A. L. Fetter and P. C. Hohenberg, in *Superconductivity*, edited by R. D. Parks (Marcel Dekker, New York, 1969), Chap. 14.
- ⁷R. Kuentzler, Y. Dossmann, S. Vilminot, and S. El Hadigui, *Solid State Commun.* **65**, 1529 (1988).
- ⁸A. P. Ramirez, R. J. Cava, G. P. Espinosa, J. P. Remeika, B. Batlogg, S. Zahurak, and E. A. Rietman, *Mater. Res. Soc. Symp. Proc.* **99**, 459 (1987).
- ⁹D. Eckert, A. Junod, A. Bezing, T. Graf, and J. Muller, *J. Low Temp. Phys.* **73**, 241 (1988).
- ¹⁰H. J. Rosen, R. M. Macfarlane, E. M. Engler, V. Y. Lee, and R. D. Jacowitz, *Phys. Rev. B* **38**, 2460 (1988).
- ¹¹S. L. Cooper, M. V. Klein, B. G. Pazol, J. P. Rice, and D. M. Ginsberg, *Phys. Rev. B* **37**, 5920 (1988).
- ¹²A. Junod, A. Bezing, T. Graf, J. L. Jorda, J. Muller, L. Antognazza, D. Cattani, J. Cors, M. Decroux, O. Fischer, M. Banovski, P. Genoud, L. Hoffman, A. A. Manuel, M. Peter, E. Walker, M. Francois, and K. Yvon, *Europhys. Lett.* **4**, 247 (1987).
- ¹³D. C. Johnston, *Phys. Rev. Lett.* **62**, 957 (1989).
- ¹⁴M. E. Reeves, Ph.D. thesis, University of Illinois, 1989.
- ¹⁵Lake Shore Cryotronics Inc., 64 E. Walnut St., Westerville, Ohio 43081.
- ¹⁶H. H. Sample, B. L. Brandt, and L. G. Rubin, *Rev. Sci. Instrum.* **53**, 1129 (1982).
- ¹⁷N. E. Phillips, R. A. Fisher, S. E. Lacy, C. Marcenat, J. A. Olsen, W. K. Ham, A. M. Stacy, J. E. Gordon, and M. L. Tan, *Physica* **148B**, 360 (1987).
- ¹⁸H. P. van der Meulen, J. J. M. Franse, Z. Tarnawski, K. Kadowaki, J. C. P. Klaasse, and A. A. Menovsky, *Physica C* **152**, 65 (1988).
- ¹⁹R. Caspary, C. D. Bredl, H. Spille, M. Winklemann, F. Steglich, H. Schmidt, T. Wolf, and R. Flükiger, *Physica C* **153-155**, 876 (1988).
- ²⁰T. Sasaki, N. Kobayashi, O. Nakatsu, T. Matsuhira, A. Tokiwa, M. Kikuchi, Y. Syono, and Y. Muto, *Physica C* **153-155**, 1012 (1988).
- ²¹E. M. Forgan, C. Gibbs, C. Greaves, C. E. Gough, F. Wellhöfer, S. Sutton, and J. S. Abell, *J. Phys. F* **18**, L9 (1988).
- ²²J. Baak, C. J. Muller, and H. B. Brom (unpublished).
- ²³S. von Molnár, A. Torressen, D. Kaiser, F. Holtzberg, and T. Penney, *Phys. Rev. B* **37**, 3762 (1988).
- ²⁴N. W. Ashcroft and N. David Mermin, *Solid State Physics* (Holt, Rinehart, and Winston, New York, 1976).
- ²⁵C. Kittel and H. Kroemer, *Thermal Physics* (Freeman, San Francisco, 1980), p. 62.
- ²⁶R. Ahrens, T. Wolf, H. Wühl, H. Rietschel, H. Schmidt, and F. Steglich, *Physica C* **153-155**, 1008 (1988).
- ²⁷S. E. Stupp and D. M. Ginsberg, *Physica C* **158**, 299 (1989).
- ²⁸F. Slakey, M. V. Klein, S. L. Cooper, E. D. Bukowski, J. P. Rice, and D. M. Ginsberg (unpublished).
- ²⁹M. B. Salamon, S. E. Inderhees, J. P. Rice, B. G. Pazol, D. M. Ginsberg, and N. Goldenfeld, *Phys. Rev. B* **38**, 885 (1988).
- ³⁰M. Tinkham, *Introduction to Superconductivity* (McGraw-Hill, New York, 1975).
- ³¹L. Krusin-Elbaum, R. L. Greene, F. Holtzberg, A. P. Malozemoff, and Y. Yeshurun, *Phys. Rev. Lett.* **62**, 217 (1989).
- ³²M. B. Salamon, in *The Physical Properties of High Temperature Superconductors*, edited by D. M. Ginsberg (World Scientific, Singapore, 1989), Chap. 2.
- ³³G. W. Crabtree, W. K. Kwok, and A. Umezawa, in *Quantum Field Theory as an Interdisciplinary Basis*, edited by F. C. Khanna, H. Umezawa, G. Kunstatter, and H. C. Lee (World Scientific, Singapore, 1988).
- ³⁴T. K. Worthington, W. J. Gallagher, D. L. Kaiser, F. H. Holtzberg, and T. P. Dinger, *Physica C* **153-155**, 32 (1988).
- ³⁵V. G. Kogan, *Phys. Rev. B* **24**, 1572 (1980).
- ³⁶L. J. Cambell, M. M. Doria, V. G. Kogan, *Phys. Rev. B* **38**, 2439 (1988).
- ³⁷P. G. de Gennes, *Superconductivity of Metals and Alloys*, translated by P. A. Pincus (Benjamin, New York, 1966), p. 71.
- ³⁸H. B. Dwight, *Tables of Integrals and Other Mathematical Data* (Macmillan, New York, 1961), Eq. 230.01.
- ³⁹J. Bardeen, D. M. Ginsberg, and M. B. Salamon, in *Novel Superconductivity*, edited by S. A. Wolf and V. Z. Kresin (Plenum, New York, 1987), p. 333.
- ⁴⁰D. E. Farrell, C. M. Williams, S. A. Wolf, N. P. Bansal, and V. G. Kogan, *Phys. Rev. Lett.* **61**, 2805 (1988).
- ⁴¹Z. Zhao and J. B. Ketterson (private communication).
- ⁴²B. Mühlischlegel, *Z. Phys.* **155**, 313 (1959).
- ⁴³L. P. Gor'kov, *Zh. Eksp. Teor. Fiz.* **10**, 833 (1960) [*Sov. Phys.—JEPT* **37**, 593 (1959)].